Bacterial Ligase D preternary-precatalytic complex performs efficient abasic sites processing at double strand breaks during nonhomologous end joining

Ana de Ory, Claudia Carabaña and Miguel de Vega [ID]*

Centro de Biología Molecular 'Severo Ochoa' (Consejo Superior de Investigaciones Científicas-Universidad Autónoma de Madrid), Nicolás Cabrera 1, 28049 Madrid, Spain

ABSTRACT

Abasic (AP) sites, the most common DNA lesions are frequently associated with double strand breaks (DSBs) and can pose a block to the final ligation. In many prokaryotes, nonhomologous end joining (NHEJ) repair of DSBs relies on a two-component machinery constituted by the ring-shaped DNA-binding Ku that recruits the multicatalytic protein Ligase D (LigD) to the ends. By using its polymerization and ligase activities, LigD fills the gaps that arise after realignment of the ends and seals the resulting nicks. Here, we show the presence of a robust AP lyase activity in the polymerization domain of *Bacillus subtilis* LigD (*Bsu*LigD) that cleaves AP sites preferentially when they are proximal to recessive 5′-ends. Such a reaction depends on both, metal ions and the formation of a Watson–Crick base pair between the incoming nucleotide and the templating one opposite the AP site. Only after processing the AP site, and in the presence of the Ku protein, *Bsu*LigD catalyzes both, the *in-trans* addition of the nucleotide to the 3′-end of an incoming primer and the ligation of both ends. These results imply that formation of a preternary-precatalytic complex ensures the coupling of AP sites cleavage to the end-joining reaction by the bacterial LigD.

INTRODUCTION

DNA double-strand breaks (DSBs) are the most deleterious DNA lesions as if unrepaired in a timely fashion can cause cell death or DNA rearrangements [1]. Such a damage can arise either during DNA replication or can be caused by environmental exposure to irradiation, chemical agents, or ultraviolet light [1]. Without a sister chromatid, as it happens during the G1 phase of the eukaryotic cell cycle and the stationary phase of many bacterial species, nonhomologous end joining (NHEJ) is the major pathway to mend DSBs whereby the DNA ends are directly joined [2,3].

In higher eukaryotes, NHEJ starts by the binding to the DNA ends of the ring-shaped Ku70/80 heterodimer that further recruits the DNA-dependent protein kinase catalytic subunit, forming a synaptic complex that holds the two ends of the broken DNA molecule together. Since the DSB termini are frequently damaged, mispaired or adducted, processing factors as nucleases (e.g. Artemis, APLF, MRN complex), phosphatases (e.g. PNPK) or polymerases (e.g. μ, λ and yeast Pol IV) remodel the ends that are finally ligated by the complex Ligase IV/XRCC4/XLF [reviewed in [4,5]]. In bacteria, NHEJ is a two-component DNA repair pathway consisting of a homodimer of Ku, homolog to its eukaryotic counterpart, which binds DSBs and recruits a multidomain protein called LigD that in most cases contains a phosphoesterase domain, a NHEJ polymerase domain (PolDom) belonging to the archaeo-eukaryotic primase superfamily [6–9], and a ligase domain (LigDom) that account for the end processing, gap filling and sealing steps, respectively [reviewed in [2,3]].

Abasic (AP) sites are the most common genomic DNA lesions frequently associated with DSBs and caused by ionizing radiation and other sources of reactive oxygen species [10–13], and by aborted base excision repair (BER) [14–17]. As the presence of AP sites near a DSB end can pose a strong block to the final ligation step during NHEJ [15,18–20], these lesions must be excised. Although AP sites had long been considered to be repaired exclusively via the BER pathway whereby the AP site is processed by an AP endonuclease, the produced 5′-dRP moiety is excised by a 5′-dRP lyase, the resulting gap is filled by a specialized DNA polymerase and the final nick is sealed by a DNA ligase, AP sites proximal to protruding 5′-ends can be specifically excised by a 5′-dRP/AP lyase activity present in the bacterial and eukaryotic Ku dimer during the NHEJ reaction [20,21]. The 5′-dRP/AP lyases exert their AP site incision through a nonmetal-dependent β-elimination mechanism whereby the protein recognizes and forms a covalent intermediate between a nucleophile (usually a lysine ε-amine) and the AP

---

site 1'-carbon that results in the cleavage of the phosphodiester bond at the 3' side, giving rise to a strand break with a ligatable 5'-phosphate and a 3'-phospho-α,β-unsaturated aldehyde (3'-PUA) end. The fact that the AP lyase activity of both, bacterial and eukaryotic Ku shows specificity for processing AP sites within a short 5' overhang is relevant for the subsequent end-joining reaction, as the resulting 5'-P end can be directly ligated to the 3'-OH terminus of an incoming primer strand [20–23]. Otherwise, incision on an AP site proximal to a 3'-protruding end would produce a ligation blocking 3'-PUA end, requiring additional processing before the sealing step. A question that remains open is how an AP site near a recessive 5'-end is excised during eukaryotic NHEJ, as the lyase activity of human Ku cannot act on AP sites embedded in the duplex region of DNA [24]. In the case of bacterial Ku, its ability to incise an AP site proximal to a recessive 5'-end remains to be elucidated.

Here, the biochemical analysis of the LigD from the gram[+] spore-forming bacterium *Bacillus subtilis* (*Bsu*LigD) shows the presence of a robust AP lyase activity in the enzyme that acts preferentially on AP sites proximal to recessive 5'-ends. Such an activity is dependent on the formation of a preternary-precatalytic complex at the DSB that would guarantee the coupling of AP sites removal to the end-joining reaction by the bacterial LigD.

MATERIALS AND METHODS

Proteins and reagents

Unlabeled nucleotides were purchased from GE Healthcare. Labeled nucleotides $[\alpha^{32}P]$-Cordycepin (3'-dATP; 3000 Ci/mmol) and $[\gamma^{32}P]$-ATP (3000 Ci/mmol) were obtained from Perkin Elmer Life Sciences. Substrates were radiolabeled at the 3' end with $[\alpha^{32}P]$-Cordycepin and terminal deoxynucleotidyl transferase (TdT) or at the 5' end with $[\gamma^{32}P]$-ATP and T4 polynucleotide kinase (T4PNK), as indicated. TdT, T4PNK, *Escherichia coli* uracil DNA Glycosylase (UDG), *E. coli* EndoIII (EndoIII), human AP endonuclease I (*h*APE1) and Ribonuclease HII (RNase-HII), were from New England Biolabs. Thrombin was obtained from Novagen. *Bsu*Ku and *Bsu*LigD were purified as described [25]. The N-terminal Ligase domain (LigDom, residues 1–320) of *Bsu*LigD was purified as described [26].

DNA substrates

The sequences of the oligonucleotides used are shown in Table 1. The 5'-FAM, 3'-Iowa Black® FQ dual labeled probe was from Integrated DNA Technologies whereas the rest of synthetic oligonucleotides were from Sigma. The dsDNA molecules were obtained by hybridizing the indicated oligonucleotides in the presence of 60 mM Tris–HCl (pH 7.5) and 0.2 M NaCl and heating to 80°C for 5 min before slowly cooling to room temperature overnight. Oligonucleotides M41 (5'-CTGUGGCTGA TGCGCAGTACGGGAATCTCCGTAGTCCGAG) and M45 (5'- CTCGGACTACGGAGATTCCCGTACTGCG CATCAGCCCCAGCAAG) were either 3'- or 5'-labeled, as indicated, and used as size markers.

Site-directed mutagenesis of *BsuLigD*

K331R, K331A, R368K and R368A *Bsu*LigD mutants were made by using the QuickChange site-directed mutagenesis kit (Agilent Technologies). Plasmid pET28a-*Bsu*LigD containing the *ykoU* gene that codes for *Bsu*LigD was used as template for the reaction [25]. The presence of the mutation and the absence of additional ones were determined by sequencing the entire gene. *Bsu*LigD mutants were expressed in *E. coli* SoluBL21™ cells (Genlantis) and further purified as described for the wild-type *Bsu*LigD [25].

AP lyase activity

A concentration of 1 nM of the indicated 2'-deoxyuridine-containing substrate was treated with *E. coli* UDG (0.2 U) for 15 min at 37°C in 30 mM HEPES (pH 7.5) and 4% glycerol to obtain natural AP sites. After incubation, the mixture was supplemented with the indicated concentration of $MnCl_2$, 10 μM of the specified nucleotide, the indicated concentration of either wild-type *Bsu*LigD, K331A, K331R, R368K, R368A mutants or LigDom and, when indicated 100 nM of *Bsu*Ku to a total volume of 12.5 μl. When pointed out, the AP site was processed with 0.2 U of either EndoIII or *h*APE1. When indicated, *Bsu*LigD was preincubated with 0.05 U of thrombin in its reaction buffer for 60 min at 20°C in a total volume of 15 μl. Samples were incubated at 30°C for the indicated times and reactions were stopped by adding freshly prepared $NaBH_4$ to a final concentration of 100 mM and incubation on ice for additional 20 min. DNA was ethanol-precipitated in the presence of 0.2 μg/ml tRNA. Reactions were analyzed by 7 M urea–20% PAGE and autoradiography.

Monitoring of the cleaved strand release

The assay was performed using as substrate 100 nM of the indicated 2'-deoxyuridine-containing fluorescently labeled probe, that was treated with *E. coli* UDG (2 U) for 60 min at 37°C in 30 mM HEPES (pH 7.5) and 4% glycerol to obtain natural AP sites. Afterwards, the mixture was supplemented with 5 mM $MnCl_2$ and 10 μM of GTP. The AP lyase activity was started with the addition of 400 nM of the wild-type *Bsu*LigD, in a final volume of 20 μl. During the incubation at 30°C, fluorescence intensity was acquired once per cycle (20 s per cycle) in a CFX384 Real Time System C1000 Thermal Cycler (Bio-Rad), in hard-Shell® 384-Well PCR Plates White Well Clear shell (Bio-Rad CN HSP-3805).

NaBH₄ trapping assay

The indicated 3'-labeled hybrid (see Table 1) was treated with 0.2 U of *E. coli* UDG for 15 min at 37°C in the presence of 30 mM HEPES (pH 7.5), 4% glycerol to obtain natural AP sites. After deglycosylation, 2 nM of the substrate was incubated for 3 min at 30°C with 95 nM of purified *Bsu*LigD, 5 mM $MnCl_2$ and 10 μM of the indicated NTP in a total volume of 12.5 μl. The Schiff base intermediate formed between the AP site and *Bsu*LigD was trapped by adding either 100 mM NaCl or freshly prepared $NaBH_4$. When indicated, *Bsu*LigD was preincubated with 0.05 U of thrombin in its reaction buffer for 20 min at 20°C in a total

Table 1. Structures and sequences of DNA substrates

Assay	Sequence of the substrates	
AP lyase activity on internal AP sites	5'-TC**U**GACTGATCACAGTGAGTAC*	
	5'-TCAG**U**CTGATCACAGTGAGTAC*	
	5'-TCA**U**ACTGATCACAGTGAGTAC*	
	5'-CTG**U**AGCTGATGCGCAGTACGGA*	
AP lyase activity on AP sites proximal to recessive 5′-ends	5'-**U**TGGAGCTGATGCGCAGTACGG* 3'-CAAC**G**ACCTCGACTACGCGTCATGCC	
	5'-**C**UGGAGCTGATGCGCAGTACGG* 3'-CAACG**A**CCTCGACTACGCGTCATGCC	
	5'-CT**U**GAGCTGATGCGCAGTACGG* 3'-CAACGA**C**CTCGACTACGCGTCATGCC	
	5'-CTG**U**AGCTGATGCGCAGTACGG* 3'-CAACGAC**C**TCGACTACGCGTCATGCC	
	5'-CTG**U**AGCTGATGCGCAGTACGG* 3'-CAACGAC**G**TCGACTACGCGTCATGCC	
	5'-^XCTG**U**AGCTGATGCGCAGTACGG* 3'-CAACGAC**A**TCGACTACGCGTCATGCC	*X=P or OH*
	5'-CTGGAGCTG**U**TGCGCAGTACGG* 3'-CAACGACCTCGAC**T**ACGCGTCATGCC	
	5'FAM-CT**U**GAGCTGATGCGCAGTACGG-3'IBFQ 3'-CAACGA**C**CTCGACTACGCGTCATGCC	
NaBH₄ trapping assay	5'-CT**U**GAGCTGATGCGCAGTACGG* 3'-CAACGA**C**CTCGACTACGCGTCATGCC	
End joining of partially complementary 3′-DNA ends	*5'-GATCACAGTGAGTACCGG 5'-^PGTACTCACTGTGAT<u>C</u> 3'-<u>C</u>TAGTGTCACTCATG 3'-CCGCATGAGTGACACTAG	
	5'-GATCACAGTGAGTACGTTG 5'-^PCT**U**GAGCTGATGCGCAGTACGG* 3'-<u>C</u>TAGTGTCACTCATG 3'- CAACGAACTCGACTACGCGTCATGCC	
End joining of partially complementary DNA ends with near terminal AP sites	5'-GATCACAGTGAGTACCTTGCTG 5'-CTG**U**AGCTGATGCGCAGTACGG* 3'-CTAGTGTCACTCATG 3'-CAACGAC**C**TCGACTACGCGTCATGCC	
	5'-GATCACAGTGAGTACGCTGCT 5'-^PCT**U**GAGCTGATGCGCAGTACGG* 3'-CTAGTGTCACTCATG 3'-CGACGACCTCGACTACGCGTCATGCC	
	5'-GATCACAGTGAGTACGCTGCT 5'-^PCT**G**GAGCTGATGCGCAGTACGG* 3'-CTAGTGTCACTCATG 3'-CGACGACCTCGACTACGCGTCATGCC	
Gap filling assay	*Cy5*-5'-GATCACAGTGAGTAC^PAACGACGGCCAGT 3'-CTAGTGTCACTCATGCTTGCTGCCGGTCA	
5'-dRP lyase activity on BER intermediates	5'-GTACTCACTGTGATC^PUGCTGATGCGCAGTACGG* 3'-CATGAGTGACACTAG.TCGACTACGCGTCATGCC	
Strand displacement assay	*Cy5*-5'-GATCACAGTGAGTAC^PCT**X**GAGCTGATGCGCAGTACGG 3'-CTAGTGTCACTCATGGGACCTCGACTACGCGTCATGCC	*X=G or THF*
	Cy5-5'-GATCACAGTGAGTAC^PCT**X**GAGCTGATGCGCAGTACGG 3'-CTAGTGTCACTCATG-GACCTCGACTACGCGTCATGCC	*X=G or THF*
Nucleotide trans-addition assay	*5'-GATCACAGTGAGTACGTTGCT 5'-^XCT**U**GAGCTGATGCGCAGTACGG 3'-CTAGTGTCACTCATG 3'-CAACGAACTCGACTACGCGTCATGCC	*X=P or OH*

U: 2'-deoxyuridine; P: 5'-phosphate group; *Cy5*: 1,1'-bis(3-hydroxypropyl)-3,3,3',3'-tetramethylindodicarbocyanine dye; *: ³²P labeled end<u>C</u>: ddCMP; FAM: 6-carboxyfluorescein; IBFQ: Iowa Black® FQ quencher; THF: tetrahydrofuran

volume of 15 μl. After incubation for 20 min on ice, samples were analyzed by 10% SDS-PAGE and visualized by either autoradiography or phosphorimager of the dried gel.

End joining of partially complementary 3′-protruding DNA ends

The reaction mixture contained, in a final volume of 12.5 μl, 30 mM HEPES (pH 7.5), 4% glycerol, 1 nM of the indicated 5′-labeled hybrid (see Table 1) and 4 nM of the specified non-labeled DNA molecule containing a protruding 3′ end, 100 nM of *Bsu*Ku and 10 μM of CTP and the indicated concentration of either the wild-type or mutant derivatives. To detect both, efficient polymerization and ligase activities 0.3 mM MnCl$_2$ was used (25). After incubation for 30 min at 30°C the reactions were stopped by adding EDTA up to 10 mM. Samples were analyzed by 7 M urea–20% PAGE and autoradiography.

End joining of partially complementary DNA ends with near terminal AP sites

To study the ability of *Bsu*LigD to coordinate AP processing with further end-joining, 1 nM of the indicated 3′-labeled downstream hybrid (see Table 1) containing an AP site proximal to the 5′-recessive end was incubated with 0.2 U of *E. coli* UDG at 37°C for 15 min, as indicated above. The deglycosylated molecule was further incubated for 30 min at 30°C with 57 nM of *Bsu*LigD and/or 114 nM of *Bsu*Ku, 10 μM of the indicated nucleotide and in the absence or presence of 4 nM of the non-labeled upstream DNA molecule (see Table 1), in a total volume of 12.5 μl. To detect both, efficient polymerization and ligase activities 0.3 mM MnCl$_2$ was used (25). Reactions were stopped by adding freshly prepared NaBH$_4$ to a final concentration of 100 mM and incubation on ice for additional 20 min. DNA was ethanol-precipitated in the presence of 0.2 μg/ml tRNA and resuspended in water. To detect the presence of a ribonucleotide embedded in the final ligation products, the indicated samples were further incubated with RNaseHII (1 U) on its reaction buffer for 30 min at 30°C. Reactions were analyzed by 7 M urea–20% PAGE and autoradiography.

To evaluate the ability of both the wild-type and *Bsu*LigD mutant K331R to perform a direct end-joining between two DNA molecules with complementary 3′-protruding ends in the presence of an AP site, 1 nM of either the indicated 3′-labeled downstream DNA molecule A containing a 2′-deoxyuridine at the third position (previously incubated with 0.2 U of *E. coli* UDG for 15 min at 37°C to obtain natural AP sites) or the indicated 3′-labeled downstream DNA molecule B containing 2′-deoxyguanosine at the third position were incubated with 4 nM of the non-labeled upstream DNA, 50 nM of either the wild-type or *Bsu*LigD mutant K331R, 100 nM *Bsu*Ku, and 4 nM of the nonlabeled upstream substrate, in the presence of 0.3 mM MnCl$_2$ and 10 μM of GTP. After incubation for 30 min at 30°C reactions were stopped by adding freshly prepared NaBH$_4$ to a final concentration of 100 mM and samples were processed as described above. To detect the presence of a ribonucleotide embedded in the final ligation products, the indicated samples were further incubated with 0.6 M NaOH for an addi-

tional 120 min at 55°C. The products of the reactions were analyzed by 7 M urea–20% PAGE and autoradiography.

Gap-filling assay

The incubation mixture contained, in 12.5 μl, 50 mM Tris–HCl (pH 7.5), 1 mM DTT, 4% glycerol, 0.1 mg/ml BSA, 5 nM of the 1-nucleotide gapped substrate (see Table 1), 50 nM GTP, 10 nM of either wild-type or mutant *Bsu*LigD proteins and 0.3 mM MnCl$_2$. After incubation for the indicated times at 30°C, reactions were stopped by adding EDTA up to 10 mM. Samples were analyzed by 7 M urea–20% PAGE and visualized using a Typhoon 9410 scanner (GE Healthcare).

Nucleotide insertion fidelity assay

The incubation mixture contained, in 12.5 μl, 50 mM Tris–HCl (pH 7.5), 1 mM DTT, 4% glycerol, 0.1 mg/ml BSA, 5 mM MnCl$_2$, 5 nM of the 1-nucleotide gapped substrate (see Table 1), 50 nM of the indicated ribonucleotide and 5 nM of *Bsu*LigD. After incubation for 5 min at 30°C, reactions were stopped by adding EDTA up to 10 mM. Samples were analyzed by 7 M urea–20% PAGE and visualized using a Typhoon 9410 scanner (GE Healthcare).

5′-dRP lyase activity on 1-nucleotide gapped BER intermediates

A concentration of 1 nM of the indicated 1-nucleotide gapped BER intermediate (upstream primer DNA with a 3′-ddCMP, see Table 1) was treated with 0.2 U of *E. coli* UDG at 37°C for 15 min in the presence of 30 mM HEPES, pH 7.5, 4% glycerol. After incubation, the mixture was supplemented with 50 nM of either the wild-type or the indicated mutant protein, in the presence of 5 mM MnCl$_2$, and 1 μM ATP, as indicated. After incubation for 10 min at 30°C, reactions were stopped by adding freshly prepared NaBH$_4$ to a final concentration of 100 mM and samples were processed as described above.

AP lyase competition assay between the wild-type and mutant derivatives

A concentration of 1 nM of the indicated 2′-deoxyuridine-containing substrate was treated with *E. coli* UDG (0.2 U) for 15 min at 37°C in 30 mM HEPES (pH 7.5) and 4% glycerol to obtain natural AP sites. After incubation, the mixture was supplemented simultaneously with 80 nM of the wild-type *Bsu*LigD, 160, 320 and 640 nM of the specified mutant protein, and 100 nM of *Bsu*Ku (when indicated) in the presence of 5 mM MnCl$_2$ and 10 μM of GTP for 15 min at 30°C. Reactions were stopped by adding freshly prepared NaBH$_4$ to a final concentration of 100 mM and samples were processed as described above.

Effect of the presence of an AP site proximal to the recessive 5′-end on the ligation reaction

The incubation mixture contained, in 12.5 μl, 50 mM Tris–HCl (pH 7.5), 1 mM DTT, 4% glycerol, 0.1 mg/ml BSA, 0.3

mM MnCl$_2$, 2 nM of the indicated 3′-labeled downstream DNA molecule, 4 nM of the indicated upstream DNA, the indicated concentration of the wild-type *Bsu*LigD and 50 nM of *Bsu*Ku. After incubation for 15 min at 30°C, reactions were stopped by adding EDTA up to 10 mM. Samples were analyzed by 7 M urea–20% PAGE and autoradiography.

Strand displacement assay

The incubation mixture contained, in 12.5 μl, 50 mM Tris–HCl (pH 7.5), 1 mM DTT, 4% glycerol, 0.1 mg/ml BSA, 5 mM MnCl$_2$, 30 nM of the indicated substrate, 300 nM of either wild-type or mutant *Bsu*LigD, and 10 μM of the four ribonucleotides. After incubation for 15 min at 30°C, reactions were stopped by adding EDTA up to 10 mM. Samples were analyzed by 7 M urea–20% PAGE and visualized using a Typhoon 9410 scanner (GE Healthcare).

AP lyase activity on gap-filled BER intermediates

A concentration of 1 nM of the indicated hybrid was treated with *E. coli* UDG (0.2 U) for 15 min at 37°C in 30 mM HEPES (pH 7.5) and 4% glycerol to obtain natural AP sites. After incubation the mixture was supplemented with EndoIII (1U) or 100 nM of the indicated *Bsu*LigD or *Bsu*LigDom. After incubation at 30°C for 30 min reactions were stopped by adding freshly prepared NaBH$_4$ to a final concentration of 100 mM and samples were processed as described above.

AP lyase activity assay on flapped 2′-deoxyuridine containing substrates

A concentration of 1 nM of the indicated 2′-deoxyuridine containing hybrids was treated with *E. coli* UDG (0.2 U) for 15 min at 37°C in 30 mM HEPES (pH 7.5) and 4% glycerol to obtain natural AP sites. After incubation the mixture was supplemented with EndoIII (0.2 U), 5 nM hAPE1 (0.2 U) or 100 nM of the indicated *Bsu*LigD or *Bsu*LigDom. After incubation at 30°C for 30 min reactions were stopped by adding freshly prepared NaBH$_4$ to a final concentration of 100 mM and samples were processed as described above.

The assays were performed three times.

RESULTS AND DISCUSSION

*Bsu*LigD cleaves internal AP sites through a nucleotide-dependent AP lyase activity

The frequency and ubiquity of AP sites, the most common genomic DNA lesions, have imposed the presence of an intrinsic AP lyase activity in a wide range of cellular proteins, both in eukaryotes and in bacteria (27–29), highlighting the importance of the correct recognition and repair of these damages. Various enzymes endowed with an AP lyase activity show a specific substrate preference. Thus, human Ku70/80 and its *B. subtilis* homologue *Bs*uKu incise preferentially AP sites within a short 5′ overhang (21,23), Pol β efficiently processes AP endonuclease-preincised 5′-dRP groups (29), and human NEIL3 has an AP lyase activity specific for single stranded DNA (30).

Recently, we have shown that *Bsu*LigD has an intrinsic 5′-dRP lyase activity at its ligase domain (LigDom; residues 1–320), that in coordination with the polymerization and ligase activities allows efficient repairing of 2′-deoxyuridine-containing DNA in an *in vitro* reconstituted BER reaction (26). The joint participation of *Bsu*LigD with the spore specific AP endonuclease (Nfo) in conferring spore resistance to ultrahigh vacuum desiccation led us to propose the existence of a minimal BER pathway in spores and constituted by the two proteins (26). The 5′-dRP lyases are a subgroup of the AP lyases, and in most cases the enzymes with a 5′-dRP lyase activity can also incise at internal AP sites (31). In this sense, *Bsu*LigD has been shown to cleave internal AP sites placed in flapped DNA molecules when the 3′-OH end of the upstream primer molecule is adjacent to the phosphodiester bond between the AP site and the next nucleotide in the downstream strand (26), being unable to act on AP sites embedded in protruding 5′-ends (21). To ascertain whether the AP lyase activity acts specifically on these substrates, or conversely it can also process internal AP sites proximal to 5′-ends, 3′-labeled 23mer single-stranded oligonucleotides with a 2′-deoxyuridine at the third (Figure 1A) or fifth (Figure 1B) position from the 5′-end were treated with *E. coli* UDG to get a natural AP site and further incubated with *Bsu*LigD, metal ions, and in the presence of the indicated ribonucleotide (see Materials and Methods). As shown, *Bsu*LigD exhibited a negligible ability to cleave the AP site on these substrates. Although those results were indicative of the incapacity of *Bsu*LigD to process 5′-end proximal AP sites, the placement of 2′-deoxyuridine at the fourth position allowed efficient cleavage of the resulting AP site, but specifically in the presence of CTP (Figure 1C). This result led us to analyze in-depth the sequence of the substrate shown in Figure 1C with the web computational engine OligoCalc (32). As shown in Figure 1D, the oligonucleotide can potentially form both, a hairpin structure and a self-dimer that resemble a dsDNA molecule with recessive 5′-ends. In this sense, the reduction of potential hairpin structures formation prevented AP site processing at the fourth position (Figure 1E). Importantly, the dsDNA structures depicted in Figure 1D would harbor a dGMP opposite the AP site.

Altogether, the above results led us to surmise that *Bsu*LigD exerts an AP lyase activity on AP sites proximal to recessive 5′-ends, such an activity being dependent on the presence of the nucleotide complementary to the one opposite the AP site. To test this hypothesis, we designed three dsDNA molecules containing an internal 2′-deoxyuridine at the fourth position from the recessive 5′-end and differing in the opposite base (A, C and G in Figure 2A, B and C, respectively). These substrates were incubated with UDG and afterwards with *Bsu*LigD in the absence/presence of the four ribonucleotides. As observed, the resulting AP site remained stable throughout the assay (lanes without ribonucleotide) and was incised by *Bsu*LigD specifically in the presence of the ribonucleotide complementary to the nucleotide opposite the AP site (U, G and C in Figure 2A, B and C, respectively), rendering a 19mer product. Although to a much lower extent, a similar result was obtained when the AP site was placed proximal to a blunt 5′-end (see Sup-
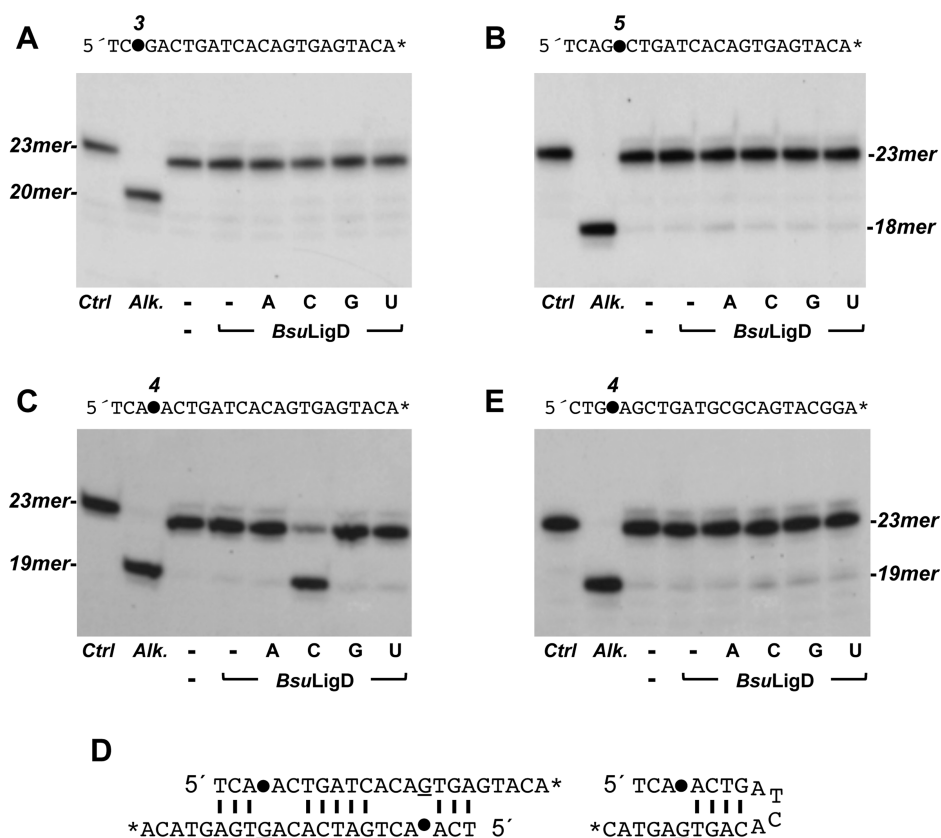
Figure 1. Analysis of the AP lyase activity of *Bsu*LigD. The ssDNA substrates containing a 2′-deoxyuridine either at the third (**A**), fifth (**B**) or fourth (**C** and **E**) position were incubated with *E. coli* UDG to create an AP site in nearly all DNA molecules. After incubation with 115 nM *Bsu*LigD in the presence of 5 mM MnCl₂ and 10 μM of the indicated nucleotide for 30 min at 30°C, samples were analyzed by 7M urea–20% PAGE and autoradiography, as described in Materials and Methods. (**D**) Potential hairpin and self-dimer structures formed by oligonucleotide shown in (C). *Alk*, alkaline hydrolysis of the AP site. The filled circle in the sequence indicates the AP site that results after treatment with *E. coli* UDG. The positions of substrate and the products are indicated. Asterisks indicate the [32P] labeled-3′ end. *Ctrl* lane corresponds to a control of the initial DNA before starting the reaction. The figure is a composite image made from different parts of the same experiment.

plementary Figure S1). This result could be indicating the requirement of a minimal length of the protruding 3′ terminus to allow the stable binding of LigD to the DNA. That the removal of the fused N-terminal His-tag from *Bsu*LigD after incubation with thrombin did not affect the AP processing by the enzyme (see Supplementary Figure S2) allows us to rule out any involvement of the tag in the AP lyase activity. To determine whether the 5′ product that results after the incision of the internal AP site by *Bsu*LigD was released after the reaction, we performed a time course assay using a fluorescently labeled DNA duplex where the AP-containing strand had the FAM fluorophore at its 5′-end whose fluorescence was quenched by the Iowa Black® FQ quencher (Integrated DNA Technologies) placed at the 3′-end (see scheme in Figure 2D and Materials and Methods). As shown in Figure 2D, the incubation of the DNA substrate with *Bsu*LigD caused a progressive increase of the fluorescence, indicating that once the AP site is cleaved the resulting 5′-FAM containing product is released. In Figure 2A, B and C, it can be observed that the reaction products show the same electrophoretical mobility to those produced after alkaline treatment of the substrate, supporting a processing of the AP site by an AP lyase activity that cleaves at the 3′-side of the AP site through a β-elimination reaction.

This mechanism involves the generation of a Schiff-base intermediate between the protein and the AP site that can be trapped *in vitro* by the strong reducing agent sodium borohydride (NaBH₄), that converts the Schiff-base to an amine, resulting in an irreversible covalent enzyme–DNA complex (31,33–36). As shown in Figure 3, *Bsu*LigD forms a stable adduct with the 3′ labeled DNA that was dependent on the presence of (i) the complementary nucleotide, (ii) the addition of NaBH₄, as no radioactive bands were detected with an equimolar concentration of NaCl and (iii) an AP site in the DNA molecule, since no complexes are formed with the uracil-containing DNA substrate. Additionally, removal of the fused N-terminal His-tag from *Bsu*LigD after incubation with thrombin gave rise to DNA–enzyme adducts with an increased electrophoretical migration, a result that allows us to assign the observed AP lyase activity to *Bsu*LigD (see Figure 3).

Internal AP processing relies on the formation of a stable *Bsu*LigD preternary-precatalytic complex

The above results indicate that efficient cleavage of the AP site depends on the formation of a Watson–Crick base pair between the correct incoming nucleotide and the templating
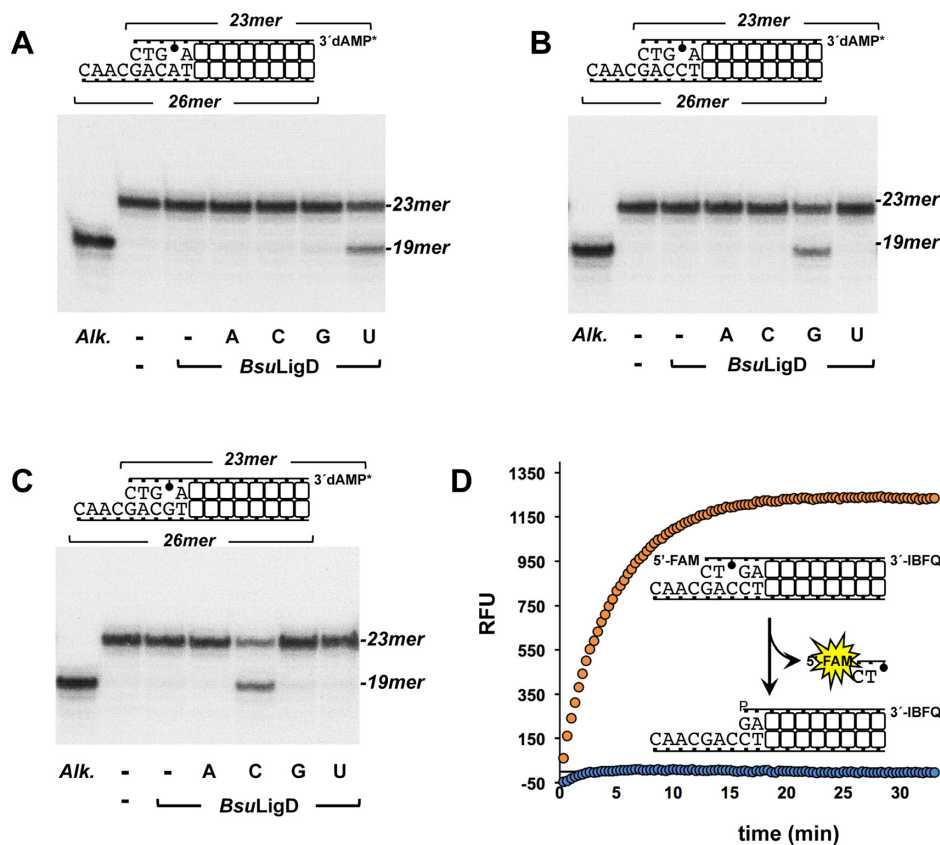
Figure 2. AP lyase activity of *Bsu*LigD on 5′-recessive ends. The assay was performed as described in Materials and Methods. The dsDNA molecules contained a 2′-deoxyuridine at the fourth position opposite to either dAMP (**A**), dCMP (**B**) or dGMP (**C**). The substrates were incubated with *E. coli* UDG to create an AP site in nearly all DNA molecules. After incubation with 115 nM *Bsu*LigD in the presence of 5 mM MnCl$_2$ and 10 μM of the indicated nucleotide for 30 min at 30°C, samples were analyzed by 7M urea–20% PAGE and autoradiography. The positions of substrate and the products are indicated. Asterisks indicate the [^{32}P] labeled-3′ end. *Alk*, alkaline hydrolysis of the AP site. The filled circle in the sequence indicates the AP site that results after treatment with *E. coli* UDG. The figure is a composite image made from different parts of the same experiment. (**D**) Time course of the AP lyase activity of *Bsu*LigD on a fluorescently labeled substrate containing a 5′-end proximal AP site. The assay was performed as described in Materials and Methods.

nucleotide opposite the AP site at the polymerization active site of *Bsu*LigD. The absence of incision activity in the presence of deoxynucleotides (see Supplementary Figure S3), would be reflecting the marked preference of *Bsu*LigD for the insertion of ribonucleotides over deoxyribonucleotides (25), as other well-characterized LigDs (2,3). Next, we analyzed the influence of the metal ions in the processing of the AP sites proximal to recessive 5′-ends. As shown in Figure 4A, the enzyme exhibited a negligible AP lyase activity without Mn^{2+}, the simultaneous addition of both, metal ions and the correct nucleotide being required to efficiently process the AP site. Importantly, the products rendered by *Bsu*LigD exhibited the same electrophoretical mobility as those released by *E. coli* EndoIII that cleaves 3′ to the AP site (37), agreeing with an intrinsic AP lyase activity in *Bsu*LigD. Interestingly, although the purified LigDom (residues 1–320) of *Bsu*LigD had been previously shown to be endowed with a 5′-dRP lyase activity (26), it was unable to incise the internal AP site on these substrates (see Supplementary Figure S4).

It has been widely documented that cleavage of an AP site by a β-elimination mechanism does not relies on metal ions, unlike hydrolytic phosphodiesterases (31). The apparent discrepancy with the results presented here has to be explained considering the structural and biochemical studies performed with *Mycobacterium tuberculosis* LigD (MtLigD) whose PolDom (Mt-PolDom) plays a major role in orchestrating the synapsis of DSBs (38,39). In the absence of a primer strand, a common fact that occurs upon DSB formation, PolDom forms a preternary-precatalytic complex with a recessive 5′-P end. The stabilization of this complex is dependent on the simultaneous presence of metal ions and the incoming nucleotide that forms a Watson–Crick base pair with the templating nucleotide nearest the recessive 5′-P end (39). The results presented above would indicate that if an AP site is proximal to the 5′-end, the preternary-precatalytic complex formation would rely on the presence of Mn^{2+} and the incoming nucleotide complementary to the templating one opposite the AP site, instead of with the nucleotide nearest the 5′-end. Here, the formation of the base pair and the presence of metal ions would confer the complex with the stability necessary to allow cleavage of the AP site, metal ions no acting as catalysts of the reaction.
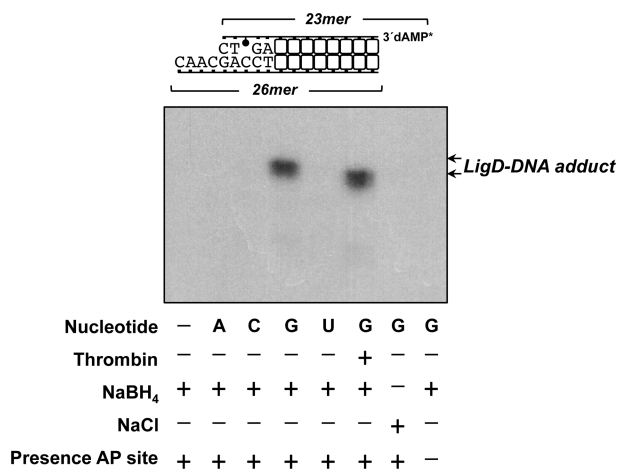
Figure 3. Formation of *Bsu*LigD-DNA adducts. Reactions were performed as described in Materials and Methods, using as substrate 2.6 nM of the 3′-[^{32}P]3′-dAMP labeled DNA either without removing the uracil (absence of AP site) or after treatment with *E. coli* UDG (presence of AP site). The substrate was incubated with 100 nM *Bsu*LigD in the presence of 10 μM of the indicated nucleotide, 5 mM MnCl$_2$ and either 100 mM NaBH$_4$ or NaCl. When indicated, protein was previously digested with 0.05 U of thrombin at 20°C for 20 min. After SDS-PAGE of the samples, protein–DNA adducts were visualized by autoradiography. Asterisks indicate the [^{32}P] labeled-3′ end. The filled circle in the sequence indicates the AP site that results after treatment with *E. coli* UDG.

The placement of the AP site determines the ingress of *Bsu*LigD into the dsDNA

Besides Mn^{2+} and nucleotide, the stability of the preternary-precatalytic complex of MtLigD was shown to rely also on the contacts established between the residues of the conserved phosphate binding pocket of Mt-PolDom (among them Lys16 and Lys26) and the 5′-P group of the recessive end (38,39). If a terminal 5′-P is lacking, the intrinsic strand displacement of LigD allowed Mt-PolDom to bind to an internal phosphate through Lys16 and Lys26 mimicking the interaction with a terminal 5′-P and maintaining the stability of the complex (39). Accordingly, the absence of a terminal 5′-P in the substrates used here could be responsible for allowing *Bsu*LigD to access to the internal AP site. To test this possibility, we evaluated the AP lyase activity of the enzyme on substrates with a 5′-P group. As shown in Figure 4B, the presence of the 5′-P neither altered the behavior of *Bsu*LigD regarding the requirements to form a preternary-precatalytic complex competent for AP site processing nor the AP lyase efficiency of the enzyme. We further analyzed the AP lyase activity of *Bsu*LigD on substrates containing an AP site placed at the first, second, third or tenth position from the recessive 5′-end (see scheme at the top of Figure 5). As expected, *Bsu*LigD processed the AP site in the first, second or third position, specifically in the presence of the correct nucleotide (CTP, UTP or GTP; panels A, B and C, respectively). The minor cleavage observed in Figure 5B and C in the presence of the non correct nucleotides could be due to the low nucleotide insertion fidelity exhibited by *Bsu*LigD (see Supplementary Figure S5). Contrarily, the nine base pairs dsDNA region would preclude *Bsu*LigD from gain access to the AP site placed at the tenth position (Figure 5D). It has been described that the presence of an

AP site can significantly alter the thermodynamic properties of a duplex destabilizing thermally and thermodynamically the DNA (40,41). Therefore, altogether the results led us to propose that the presence of an AP site proximal to a 5′-end could promote the partial melting of the recessive terminus. This fact would hinder the interaction of PolDom with the terminal 5′-P group that is observed when the 5′-end is perfectly paired (39), allowing LigD to access into dsDNA until reaching the AP site.

To determine the role of the 5′-P binding pocket of *Bsu*LigD in its AP lyase activity, residue Lys331, the homologous to Mt-LigD Lys16 (25) was changed either to alanine or to arginine, and the resulting K331A and K331R mutants were overproduced and purified as described in Materials and Methods. As shown in Figure 6A (see also Supplementary Figure S6), mutants K331R and K331A were neither able to process the AP site proximal to the recessive 5′-end nor form a covalent complex with the DNA after reduction with NaBH$_4$ (Figure 6B). We further evaluated the effect of *Bsu*Ku on the AP lyase activity of the wild-type and the mutant LigDs (Figure 6C). As shown, whereas *Bsu*Ku exhibits a negligible AP lyase activity on the recessive 5′-end, as its eukaryotic homolog (24), its binding to the DNA stimulates the AP lyase activity of the wild-type *Bsu*LigD, in good agreement with the role of *Bsu*Ku in recruiting LigD to the ends of a DSB (see also Supplementary Figure S7). These results, together with the incapacity of *Bs*uLigD and proficiency of *Bsu*Ku to act on AP sites near a protruding 5′-end (21), strongly suggests a complementary role for these two proteins in processing AP sites. Regarding mutants K331R and K331A, they were unable to process the AP site even in the presence of *Bsu*Ku (Figure 6C). To rule out a potential misfolding of the mutant proteins as responsible for the absence of AP lyase activity we evaluated to what extent their polymerization and ligase activities were affected. To that, we performed a gap-filling assay using a 1-nucleotide gapped molecule as substrate (Figure 7A). As shown, mutant K331R displayed a wild-type polymerization and ligation activities. Contrarily, the absence of an electropositive charge in mutant K331A slightly reduced the nucleotide insertion efficiency of the enzyme, in agreement with the role of Lys331 in 5′-P binding. We further studied the ability of the mutant proteins to perform end-joining, a demanding reaction where the enzyme once bound to the recessive 5′ ends has to connect partially complementary 3′-protruding DNA termini coming from independent DNA molecules to form a gap-like synaptic intermediate (42). To that, the two 3′ protruding DNA molecules depicted in Figure 7B (note that only one of the molecules is 5′-labeled, see also Table 1) and whose synapsis would render a 1-nucleotide gapped molecule, were simultaneously incubated with either the wild-type or mutant derivatives, CTP to allow the gap filling reaction, 0.3 mM Mn^{2+} [a metal concentration that allows efficient polymerization, ligase and AP lyase activities [(25), see also Supplementary Figure S3] and in the presence/absence of *Bsu*Ku. As shown in Figure 7B, the wild-type protein required the previous binding of *Bsu*Ku to the DSB to extend the 3′-end of the labeled strand, indicating that unlike Mt-PolDom, *Bsu*LigD is unable to accomplish the synapsis of the two ends by itself (25). This difference between the two proteins is most probably because
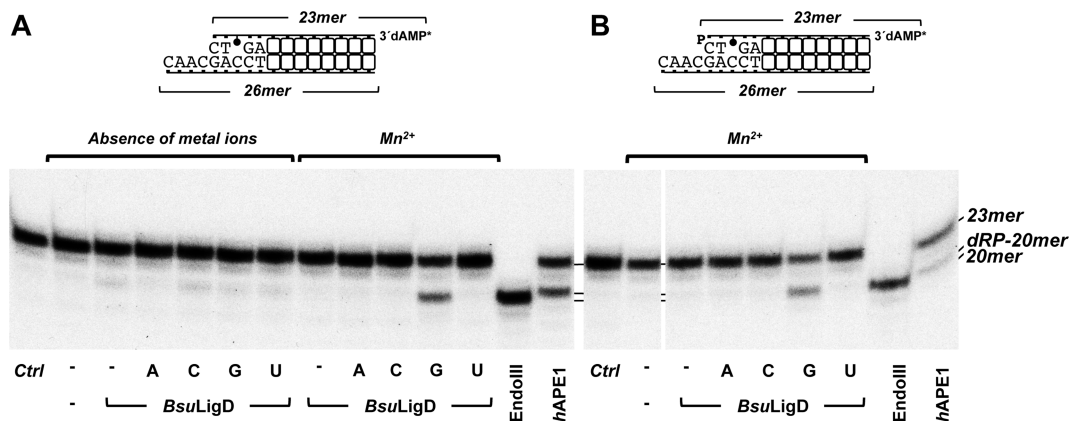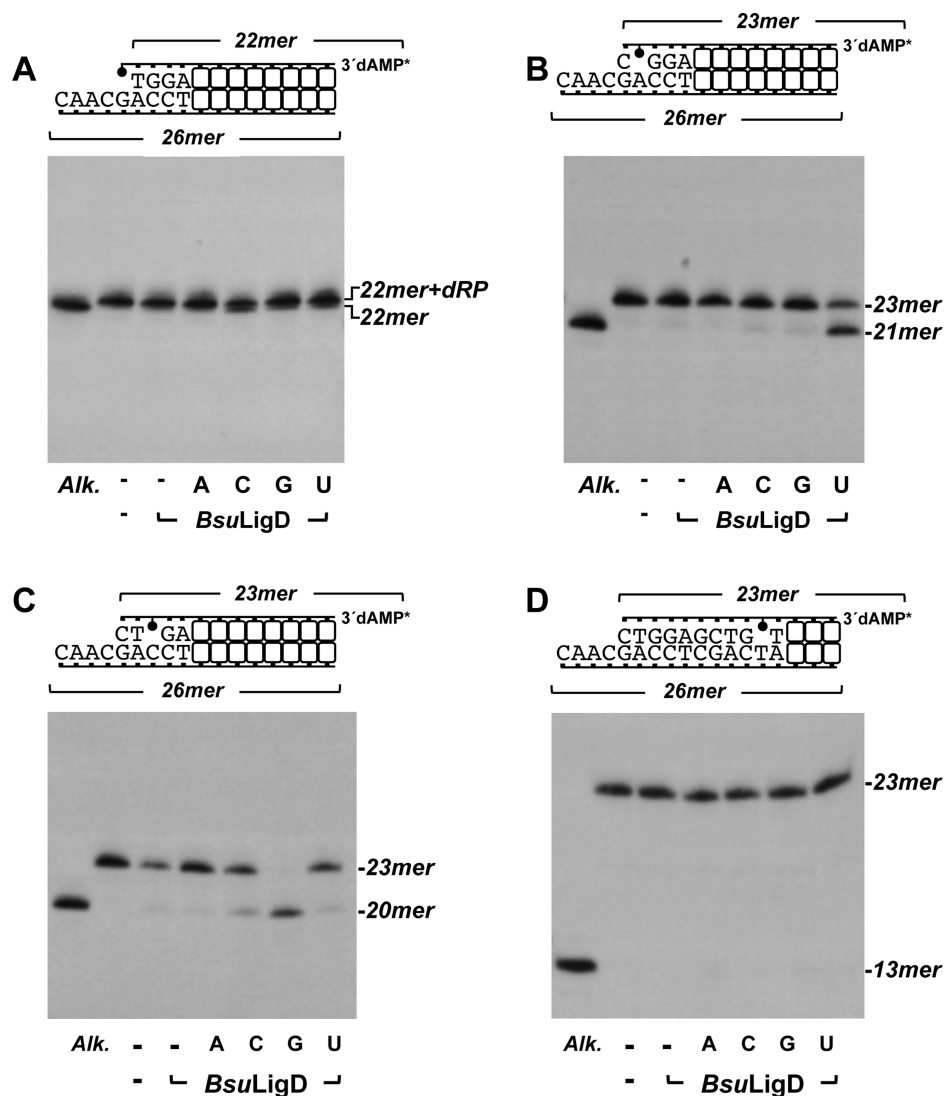
Figure 4. Effect of metal ions and 5′-P group in the AP lyase activity of *Bsu*LigD. (**A**) Effect of metal ions. The assay was performed as described in Materials and Methods. The substrates containing a 2′-deoxyuridine at the third position were incubated with *E. coli* UDG to create an AP site in nearly all DNA molecules. After incubation for 30 min at 30°C of the AP-containing molecules with either 50 nM *Bsu*LigD, 0.2 U of *E. coli* EndoIII or *h*APE1, in the absence or presence of 5 mM MnCl₂ and 10 μM of the indicated nucleotide, samples were analyzed by 7M urea–20% PAGE and autoradiography. (**B**) *Effect of the 5′-P group.* The assay was performed as indicated in (A), incubating 1 nM of the *E. coli* UDG treated 5′-P-containing DNA depicted in top of the figure, in the presence of 5 mM MnCl₂, either 50 nM *Bsu*LigD, 0.2 U of *E. coli* EndoIII or 0.2 U of *h*APE1 and 10 μM of the indicated nucleotide. Positions corresponding to the products are indicated. Asterisks indicate the [³²P] labeled-3′ end. *Ctrl* lane corresponds to a control of the initial DNA before starting the reaction. The filled circle in the sequence indicates the AP site that results after treatment with *E. coli* UDG. The figure is a composite image made from different parts of the same experiment.

Mt-LigD contains a prominent surface β-hairpin structure called loop 1 that interacts with the 3′-protruding ends in a NHEJ complex and maintains the synapsis between the two DNA termini (42). The shorter loop 1 in *Bsu*LigD could be impeding the enzyme to form a synaptic complex, relying on the previous DNA binding of Ku to accomplish the NHEJ reaction. As shown in Figure 7B, in the presence of Ku, mutant K331R and to a lower extent K331A carried out the template-directed insertion of CMP at the 3′-end of the labeled strand, indicating that synapsis between the two molecules took place (the absence of elongation products without the nonlabeled substrate rules out a potential terminal transferase activity as responsible for the extension of the labeled primer strand, see Supplementary Figure S8). After addition of the nucleotide, the resulting nick was sealed by the ligase activity to render a repaired (ligated) product. These results indicate, on the one hand that *Bsu*Ku recruits the mutant proteins to the DNA ends, and on the other hand that their polymerization and ligase activities, mainly in mutant K331R, are not affected. To compare the DNA binding efficiency of the wild-type and K331R and K331A mutants to a recessive 5′-end containing an AP site at the third position, we carried out a competition assay where the wild-type enzyme and the mutant proteins compete for the DNA (Figure 7C). To that, the DNA substrate was simultaneously incubated with a fixed concentration of the wild-type enzyme (80 nM), the indicated concentrations of the corresponding mutant protein (160–640 nM) and in the absence (upper panel) or presence (lower panel) of 100 nM *Bsu*Ku. As it can be observed, in both cases the presence of a 8-fold higher concentration (640 nM) of mutant protein reduced 2- (in the absence of Ku) and 4-fold (in the presence of Ku) the activity of the wild-type protein, a result that reflects a deficient DNA binding capacity of both mutants to the AP-containing 5′ recessive end, agreeing with a binding role to internal phosphates for this residue, as previously reported for the homologous Mt-PolDom Lys16 (42). However, not even the incubation of the DNA with 640 nM of the mutant proteins in the presence of Ku rendered any degradation product. Thus, the catalytic behavior of Lys331 in the AP lyase activity, together with the incapacity of the 5′-dRP/AP lyase activity of the purified LigDom (26) to incise on the AP site proximal to a recessive 5′-end (see Supplementary Figure S4) strongly suggest the presence of an additional AP lyase activity at the polymerization domain of *Bsu*LigD that would act specifically on these DNA substrates with Lys331 residue acting as the main nucleophile. Importantly, the new 5′-P end that results after the cleavage of the AP site would be already bound to the 5′-P binding pocket, *Bsu*LigD being ready to catalyze the further NHEJ reaction.

The preternary complex enables efficient coordination between AP site processing and further end-joining

Once proved the capacity of *Bsu*LigD to cleave AP sites proximal to recessive 5′-ends through the formation of a preternary-precatalytic complex, we analyzed its ability to coordinate the AP processing with the *in trans* extension of an incoming primer and the final ligation of the break. To that, a NHEJ reaction was set up using the substrates depicted in the scheme of Figure 8 (see also Materials and Methods and Table 1). Thus, the 3′-labeled downstream molecule harbors an AP site at the fourth position of the 5′-recessive end that, only after its precise processing by the AP lyase activity should result in a molecule with a 3′-protruding end partially complementary to the upstream non-labeled molecule, the synapsis of both substrates rendering a 1-nucleotide gapped molecule with a templating dCMP. In agreement with the results previously shown in Figure 6C, *Bsu*Ku exhibited a negligible AP lyase activity on these DNA molecules (Figure 8, lanes *a*, *b*, *h* and *i*). *Bsu*LigD did not process the AP site with the incorrect
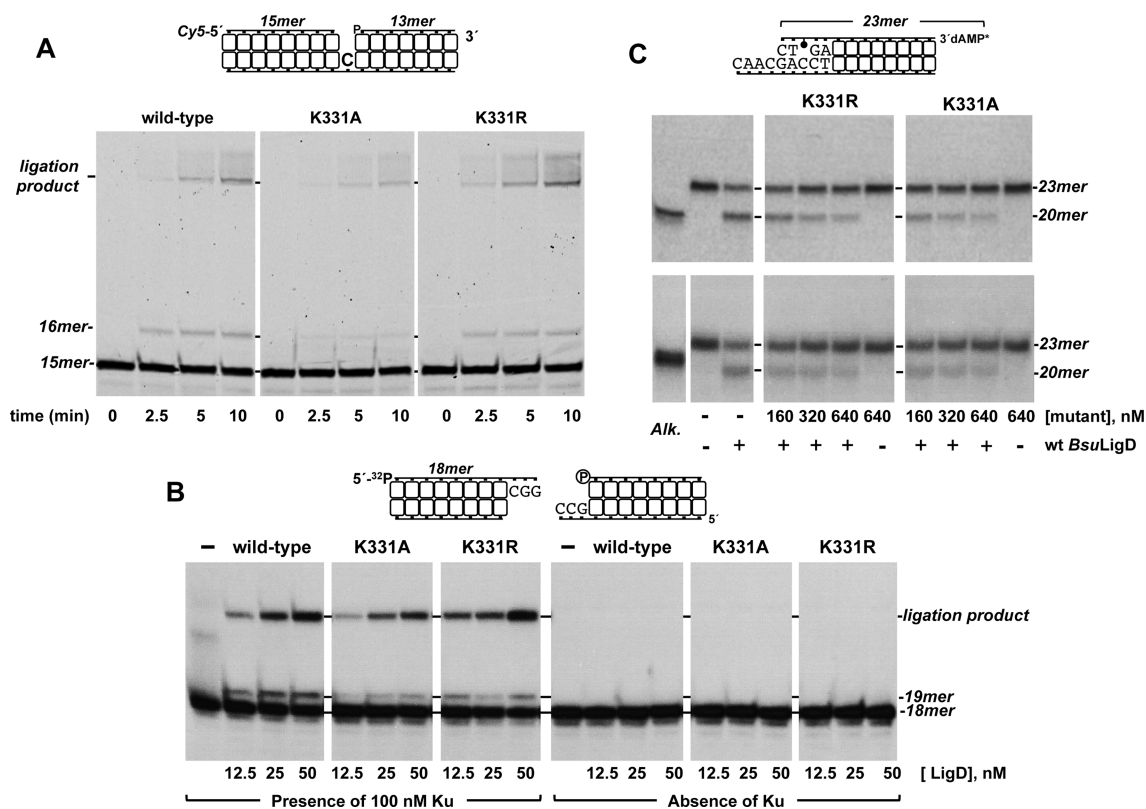
Figure 5. Activity of *Bsu*LigD on AP sites proximal to the recessive 5′-end. The assay was performed as described in Materials and Methods. The substrates containing a 2′-deoxyuridine at the first (**A**), second (**B**), third (**C**) and tenth (**D**) position from the 5′-end were incubated with *E. coli* UDG to create an AP site in nearly all DNA molecules. After incubation of the AP-containing molecules with 115 nM *Bsu*LigD in the presence of 5 mM MnCl$_2$ and 10 μM of the indicated nucleotide for 30 min at 30°C, samples were analyzed by 7M urea–20% PAGE and autoradiography. The positions corresponding to substrate and the products are indicated. Asterisks indicate the [^{32}P] labeled-3′ end. *Alk*, alkaline hydrolysis of the AP site. The filled circle in the sequence indicates the AP site that results after treatment with *E. coli* UDG. The figure is a composite image made from different parts of the same experiment.

ATP (lanes *c* and *d*), not even in the simultaneous presence of *Bsu*Ku (lanes *e* and *f*). As expected, addition of GTP allowed *Bsu*LigD to cleave the 35% of the AP sites of the downstream molecule (lane *j*). The apparent loss of activity in the presence of the non-labeled upstream DNA (only 10% of the substrate is processed by *Bsu*LigD) could be due to the unspecific binding of *Bsu*LigD to this substrate (lane *k*). When *Bsu*Ku was added to the reaction, it recruited *Bsu*LigD to the ends, as described (25), enhancing 1.47-fold the inherent AP lyase activity of the enzyme, that now incises on the 51% of the initial molecules (compare lanes *j* and *l*). Importantly, the simultaneous presence of *Bsu*LigD, *Bsu*Ku, GTP and upstream DNA increases the AP lyase efficiency of *Bsu*LigD, that processes 66% of the AP sites, giving rise to a ligation product (lane *m*) with an electrophoretic mobility slightly lower than the 41mer

marker, ruling out a direct ligation of the 3′ end of the primer to the 5′-P that results after cleavage at the AP site. Further treatment of the ligation product with the endoribonuclease RNaseHII, that nicks 5′ to a ribonucleotide within the context of a duplex DNA (43), rendered a 20mer product (lane *n*). The results indicate that LigD catalyzed the *in trans* addition of the GMP already paired with the templating dCMP in the preternary complex, to the 3′-OH of the incoming primer strand before ligation to the 5′-P that arises after the AP cleavage. To evaluate the ability of both the wild-type and mutant K331R to perform a direct end-joining between two DNA molecules with complementary 3′-protruding ends in the presence of an AP site, we performed a NHEJ assay where the 3′-protruding end of the upstream DNA can be perfectly paired to the 3′-protruding end of the downstream substrates A and B (Fig-

Figure 6. AP lyase activity of *Bsu*LigD mutants. The assays were performed as described in Materials and Methods. The substrate containing a 2′-deoxyuridine at the third position was incubated with *E. coli* UDG to create an AP site in nearly all DNA molecules. (**A**) *AP lyase activity in the absence of BsuKu*. After incubation of 1 nM of the UDG-treated DNA with 50 nM of either the wild-type or *Bsu*LigD mutants, 5 mM $MnCl_2$ and 10 μM of the indicated nucleotide for 30 min at 30°C, samples were analyzed by 7M urea–20% PAGE and autoradiography, as described. The positions of substrate and the products are indicated. *Ctrl* lane corresponds to a control of the initial DNA before starting the reaction. *Alk*, alkaline hydrolysis of the AP site. The figure is a composite image made from different parts of the same experiment. (**B**) *Formation of BsuLigD-DNA adducts*. Reactions were performed as described in Materials and Methods, using as substrate 2.6 nM of the UDG-treated DNA, 100 nM of either the wild-type or *Bsu*LigD mutants,10 μM of GTP and 5 mM $MnCl_2$. When indicated, proteins were previously digested (+) with 0.05 U of thrombin at 20°C for 20 min. After SDS-PAGE of the samples, protein-DNA adducts were visualized by autoradiography. Asterisks indicate the [^{32}P] labeled-3′ end. (**C**) *AP lyase activity in the presence of BsuKu*. The assay was performed as in (A) in the presence of 10 μM GTP and in the absence (–) or presence (+) of 100 nM of *Bsu*Ku. The figure is a composite image made from different parts of the same experiment. The filled circle in the sequence indicates the AP site that results after treatment with *E. coli* UDG.

ure 9). Downstream substrate A harbors an AP site at the third position respect to the recessive 5′-P end, therefore, the upstream DNA could pair either to the three nucleotides of the 3′-protruding end of molecule A to give rise to a 45mer long product after the *in trans* addition of GMP and ligation reactions, or to the six nucleotides of the 3′-protruding end of molecule A that results after the AP cleavage. In the latter case, the resulting product would be 42mer long after the *in trans* addition and ligation reactions. In substrate B, the absence of an AP site would allow exclusively the formation of the three base pairs described above, giving rise to the final 45mer long product after the *in trans* addition and ligation reactions. As shown in Figure 9, in the presence of the downstream molecule A, the wild-type enzyme rendered a 42mer product (lane *a*). Further alkaline treatment caused the hydrolysis of the ligation product, indicating the presence of a ribonucleotide embedded into the DNA strand (lane *b*), and agreeing with a previous cleavage at the AP site followed by the *in trans* addition of GMP and final liga-

tion steps. In the case of mutant K331R no ligation products were detected (lanes *c* and *d*). Unlike with substrate A, the presence of the downstream molecule B allowed the wild-type and mutant K331R to give rise to a 45mer long product (lanes *e* and *g*) containing an internal GMP (lanes *f* and *h*), indicating, on the one hand that both the wild-type and mutant K331R catalyzed the *in trans* addition of GMP before the sealing step, and on the other hand suggesting that the presence of an AP site proximal to the 5′-end impairs the direct ligation of both molecules, as previously described [(22), see also Supplementary Figure S9], compelling LigD to cleave the AP site.

Altogether, the results presented here indicate that if an AP site is proximal to the 5′-end, *Bsu*LigD forms an internal preternary-precatalytic complex that guarantees both, efficient processing of AP sites proximal to a recessive 5′-P and further end-joining to an incoming primer molecule. A scheme of the proposed catalytic cycle when an AP site is close to the recessive 5′-end is drawn in Figure 10. Thus,

Figure 7. Polymerization, ligation and DNA binding activities of mutants at residue Lys331 of *Bsu*LigD. (**A**) *Gap-filling and ligation activities of mutants at residue Lys331 of BsuLigD*. The assay was carried out as described in Materials and Methods in the presence of 5 nM of the depicted 1-nucleotide gapped molecule, 10 nM of either the wild-type or *Bsu*LigD variants and 50 nM GTP. Samples were analyzed by 7 M urea–20% PAGE and visualized using a Typhoon 9410 scanner (GE Healthcare). Position of products is indicated. The figure is a composite image made from different parts of the same experiment. (**B**) *End joining of partially complementary 3′-protruding DNA ends by mutants at residue Lys331 of BsuLigD.* The assay was carried out as described in Materials and Methods by incubating 1 nM of the ³²P 5′-labeled hybrid depicted on top of figure, in the presence of the indicated concentrations of either the wild-type or *Bsu*LigD variants, 4 nM of the nonlabeled hybrid, 10 μM of CTP and in the absence/presence of 100 nM *Bsu*Ku. After incubation for 30 min at 30°C, the elongation and ligation products were analyzed by 7 M urea–20% PAGE and autoradiography. Position of products is indicated. The figure is a composite image made from different parts of the same experiment. (**C**) *AP lyase competition assay between the wild-type and mutant derivatives.* The assay was performed as described in Materials and Methods. The depicted substrate containing a 2′-deoxyuridine at the third position was incubated with *E. coli* UDG to create an AP site in nearly all DNA molecules. The wild-type *Bsu*LigD (80 nM) was incubated simultaneously with the indicated concentration of the specified mutant protein, in the absence (upper panel) or presence (lower panel) of 100 nM *Bsu*Ku for either 30 min (upper panel) or 15 min (lower panel) at 30°C. After incubation samples were analyzed by 7M urea–20% PAGE and autoradiography, as described in Materials and Methods. The positions of substrate and the products are indicated. Asterisk indicates the [³²P] labeled-3′ end. *Alk*, alkaline hydrolysis of the AP site. Full circle, AP site that results after treatment with *E. coli* UDG. The figures are composite images made from different parts of the same experiments.

after the breakage, the DNA end is threaded through the open ring-like structure of the *Bsu*Ku dimer (Figure 10A). The location of the AP site proximal to the 5′-end could promote the partial melting of the 5′-end making the AP site accessible. Thus, after its recruitment by *Bsu*Ku, *Bsu*LigD would form a complex with the DNA, most probably implying the interaction of Lys331 with one of the phosphates of the phosphodiester bond between the AP site and the next 3′ nucleotide, as described in Mt-PolDom preternary complex (39) (Figure 10B), as well as by residues that intercalate into the downstream annealed DNA interface through the formation of hydrogen bond contacts with the ribose of the ultimate base of the downstream strand (see Supplementary text and Supplementary Figure S10). Such interactions would allow *Bsu*LigD to place, at its polymerization catalytic site, the templating nucleotide opposite the AP site that would direct the binding of the complementary ribonucleotide, forming a Watson–Crick base pair (Figure

10C). The presence of metal ions would ensure that the correct incoming nucleotide is bound at the active site before resection of the AP site. Once the preternary-precatalytic complex is stabilized, the protein would incise at the AP site most probably through Lys331, releasing the cleaved strand and giving rise to a new 5′-P end that would keep the contacts with the phosphate binding pocket (Figure 10D). As soon as the primer molecule reaches the PolDom of *Bsu*LigD and the resulting ternary complex has been formed, *Bsu*LigD catalyzes the *in trans* addition of the nucleotide to the 3′-end of the incoming primer and the final ligation of both ends, as described for Mt-PolDom (39).

As mentioned before, *Bsu*LigD has been proposed to play a role in the BER pathway as its deletion sensitizes the spores to UHV desiccation, a treatment that causes single stranded breaks, and its role is epistatic with the spore-specific AP endonuclease Nfo. The enzyme was shown to be perfectly suited to account for efficient repairing of 2′-
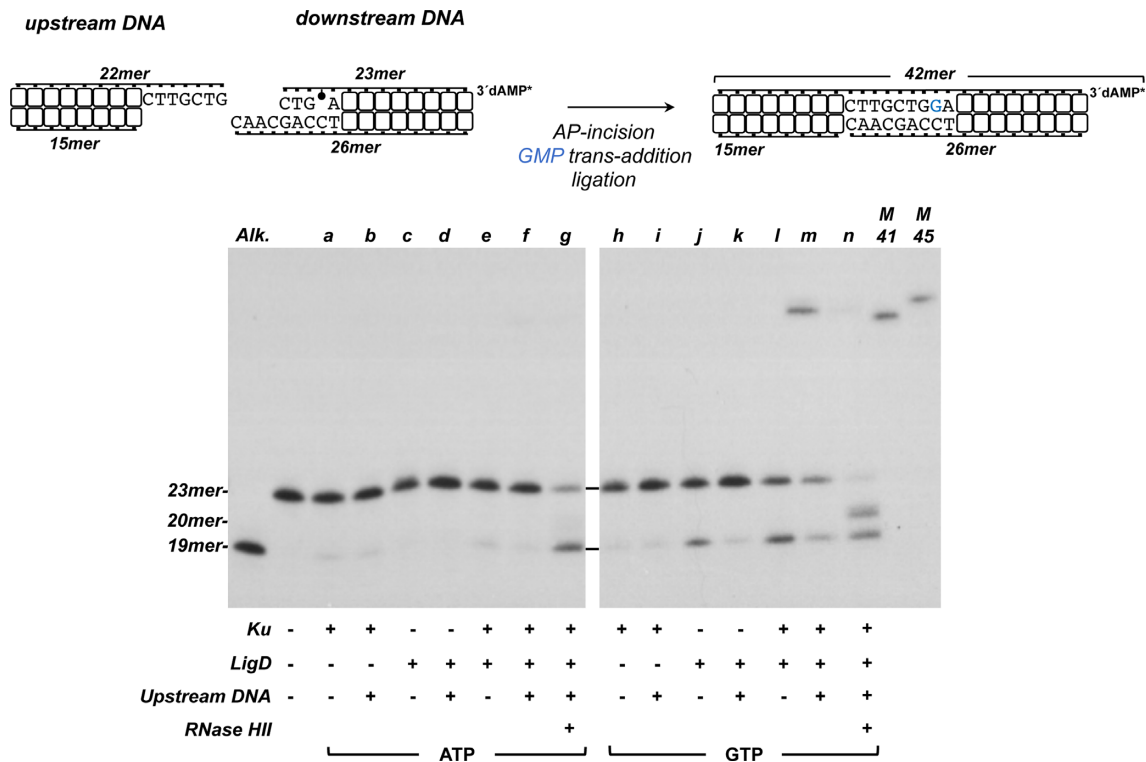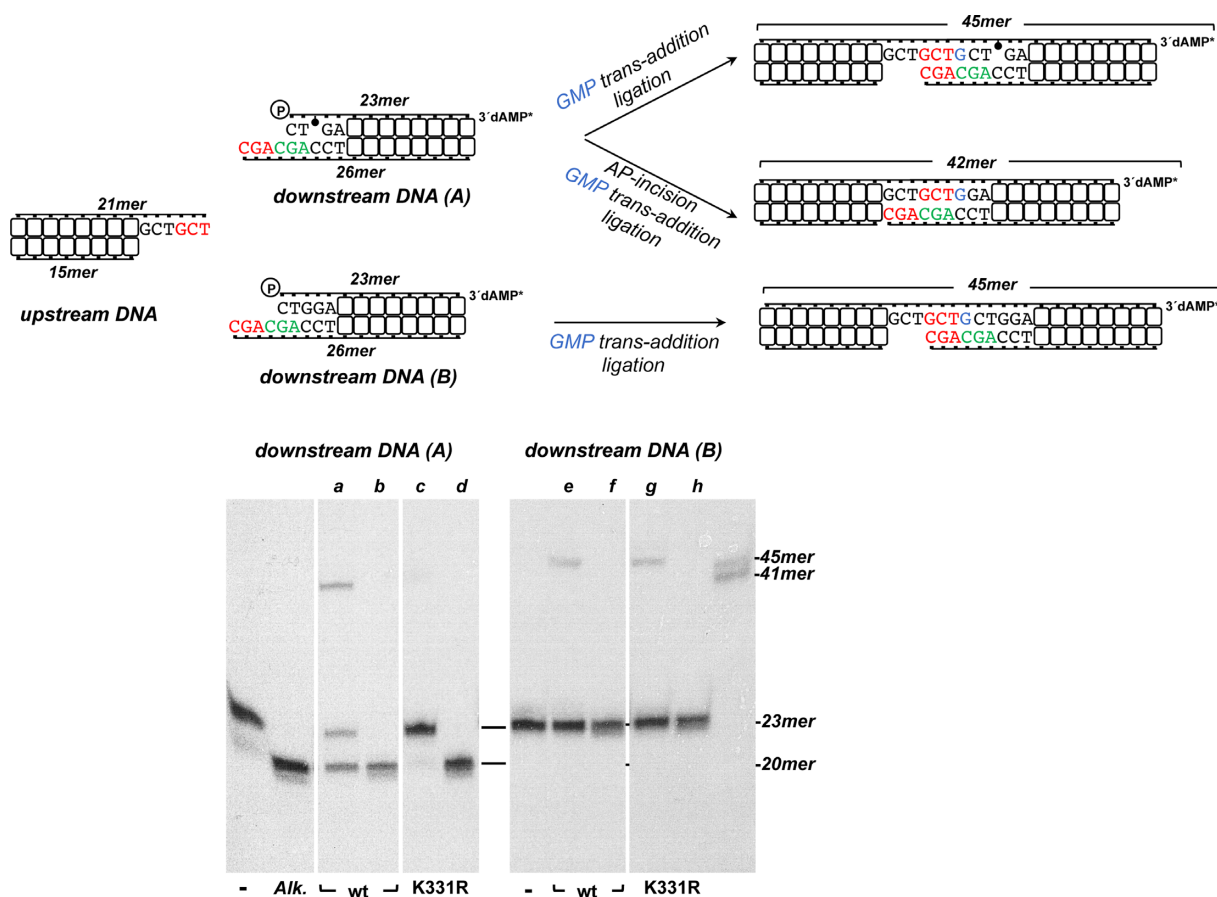
Figure 8. End joining of partially complementary DNA ends with near terminal AP sites. The assay was carried out as described in Materials and Methods. 1 nM of the 3′-labeled substrate containing a 2′-deoxyuridine at the fourth position was incubated with *E. coli* UDG to create an AP site in nearly all DNA molecules. When indicated, the AP-containing molecules were incubated with 57 nM of the wild-type *Bsu*LigD, 114 nM *Bsu*Ku, and 4 nM of the nonlabeled upstream substrate, in the presence of 0.3 mM MnCl$_2$ and 10 μM of the specified nucleotide. After incubation for 30 min at 30°C, the indicated sample was incubated with RNaseHII for an additional 30 min. The products of the reactions were analyzed by 7 M urea–20% PAGE and autoradiography (M41 and M45: 41mer and 45mer oligonucleotides used as size marker; *Alk.* alkaline hydrolysis of the UDG-treated DNA). The lengths of the labeled substrate and the degradation and ligation products are indicated. The figure is a composite image made from different parts of the same experiment.

deoxyuridine-containing DNA in an *in vitro* reconstituted BER through the coordinated action of its inherent polymerization, ligase and 5′-dRP lyase activities (26). Interestingly, unlike other polymerases involved in gap-filling and 5′-dRP release during BER, as eukaryotic polymerases β (44), ι (45), λ (46) and θ (47), the excision of the 5′-dRP group by *Bsu*LigD was dependent on the previous filling of the gap (26). Based on the results presented here, it was tempting to speculate that excision of the 5′-dRP group in a gap by LigD would require also the previous formation of a ternary-precatalytic complex. To test this hypothesis the protein was incubated with a dsDNA molecule containing a 1-nucleotide gap flanked by a 5′-dRP group and a 3′ddC to prevent insertion of the incoming nucleotide, and in the presence of Mn^{2+} ions and each of the four ribonucleotides. As shown in Supplementary Figure S11, the wild-type enzyme released the 5′-dRP group specifically in the presence of ATP, indicating that excision of the 5′-dRP moiety during BER relies also on the formation of a Watson–Crick base pair between the incoming nucleotide and the templating one opposite the 5′-dRP group. In agreement with the results presented above, none of the mutant proteins were endowed with a 5′-dRP lyase activity, a result that supports Lys331 as the residue responsible for the 5′-dRP lyase activity.

Our previous studies with the independently expressed LigDom of *Bsu*LigD showed, as in other ATP-dependent DNA ligases as those from bacteriophages T4 and T7 (48,49) the presence of a 5′-dRP/AP lyase activity since the domain could release the dangling 5′-dRP group from a filled gap in a metal-independent manner (26). Here, we have found the ability of *Bsu*LigD to act on natural AP sites proximal to recessive 5′-ends. That the independently expressed LigDom is not able to act on these AP sites, together with the absolutely essential role of the PolDom residue Lys331 in the AP lyase activity on those substrates has led us to infer the presence of an additional AP lyase activity acting on internal AP sites proximal to a 5′-end. As the AP lyase activity of LigDom is very proficient in cleaving AP sites, specifically on DNA substrates where the 3′-end of the upstream strand is adjacent to the phosphodiester bond between the AP site and the next nucleotide in the downstream strand (26), it was tempting to speculate that mutants K331R and K331A could be able to incise on this kind of DNA substrates, as they harbors an intact LigDom. To test this hypothesis, we performed the experiments shown in Figure 11. In the left, we used as substrate a DNA hybrid mimicking the situation previous to the 5′-dRP release, with the 3′-OH end of the upstream strand adjacent to the last phosphodiester bond between the penultimate 5′-nucleotide and the terminal 5′-dRP group of the down-

Figure 9. Effect of the AP site in end joining of partially complementary DNA ends with near terminal AP sites. The assay was carried out as described in Materials and Methods, incubating 1 nM of either the 3′-labeled downstream DNA A (presence of an AP site at the third position) or B (absence of AP site) with 50 nM of either the wild-type or the *Bsu*LigD mutant K331R, 100 nM *Bsu*Ku, and 4 nM of the nonlabeled upstream substrate, in the presence of 0.3 mM MnCl₂ and 10 μM of GTP. After incubation for 30 min at 30°C samples *b*, *d*, *f* and *h* were incubated with 0.6 M NaOH for an additional 120 min at 55°C. The products of the reactions were analyzed by 7 M urea–20% PAGE and autoradiography (M41 and M45: 41mer and 45mer oligonucleotides used as size marker; *Alk*. alkaline hydrolysis of the UDG-treated DNA). The lengths of the labeled substrate and the degradation and ligation products are indicated. The figure is a composite image made from different parts of the same experiment.

stream strand. As it can be observed, with this substrate the LigDom as well as mutant K331R and, to a lower extent mutant K331A exhibited the lyase activity. Similarly, in the experiment shown in the right, we used the flapped DNA structure depicted in top of the figure and containing a 2′-deoxyuridine at position 19 of the 35mer downstream oligonucleotide. This DNA was previously treated with *E. coli* UDG to get a natural AP site. Incubation of this substrate with *h*APE1 rendered a 16mer product with a 5′-dRP end as this enzyme is a metal-dependent AP endonuclease that hydrolyzes the phosphodiester bond 5′ to the AP site. Conversely, *E. coli* EndoIII incised at the 3′ side by its AP lyase activity leaving a product that migrates faster due to the presence of a 5′-P. As it can be observed, the wild-type enzyme, the LigDom and mutant K331R rendered a product with the same electrophoretical mobility to that produced by EndoIII, consistent with a cleavage at the 3′ side to the AP site. Altogether, the results strongly support the presence of two AP lyase activities in the enzyme showing a grade of specialization that seems to be dependent on the DNA structure.

In eukaryotes, PolX members as Polμ and Polλ are the NHEJ polymerases of choice. Although evolutionary unrelated, they share functional and structural features with bacterial PolDom, such as structurally superimposable catalytic active sites (50), stimulation of the polymerization activities by their cognate Ku (25,50–52), and preferential binding to a recessive 5′-P end. In family X DNA polymerases recognition of the 5′-P is accomplished also by an electropositive phosphate binding pocket, present in their 8-kDa domain, and formed in Polλ by residues Arg275, Arg308, and Lys312 (53,54) (see Supplementary Figure S12). As mentioned before, Polλ is also endowed with an inherent 5′-dRP lyase that excises the 5′-dRP moiety at least in reconstituted *in vitro* BER reactions (46). Interestingly, the Polλ 5′-P binding pocket residue Lys312 is the main nucleophile responsible for the 5′-dRP lyase (46), agreeing with a convergent evolution of the members of the bacterial and eukaryotic NHEJ polymerases to use similar catalytic mechanisms, as previously suggested (2). Thus, by analogy with *Bsu*LigD, it is tempting to speculate a role of Polλ in processing AP sites at DSBs during eukaryotic NHEJ.
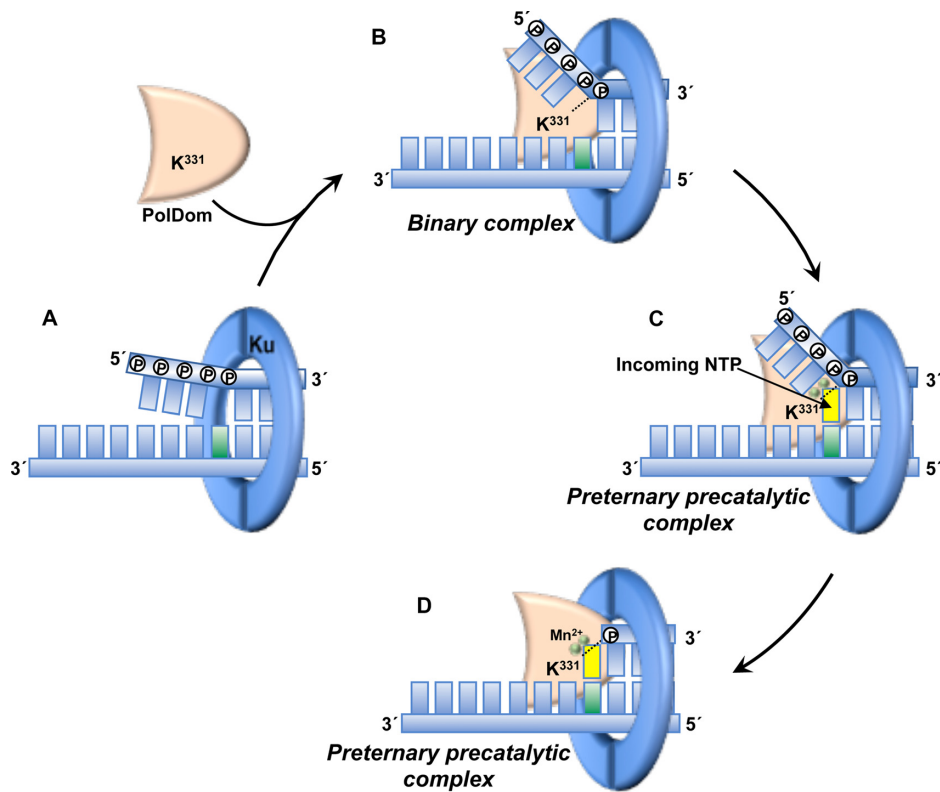
Figure 10. Bacterial PolDom preternary-precatalytic complex formation when an AP site is proximal to the recessive 5′-end. For details see the main text.
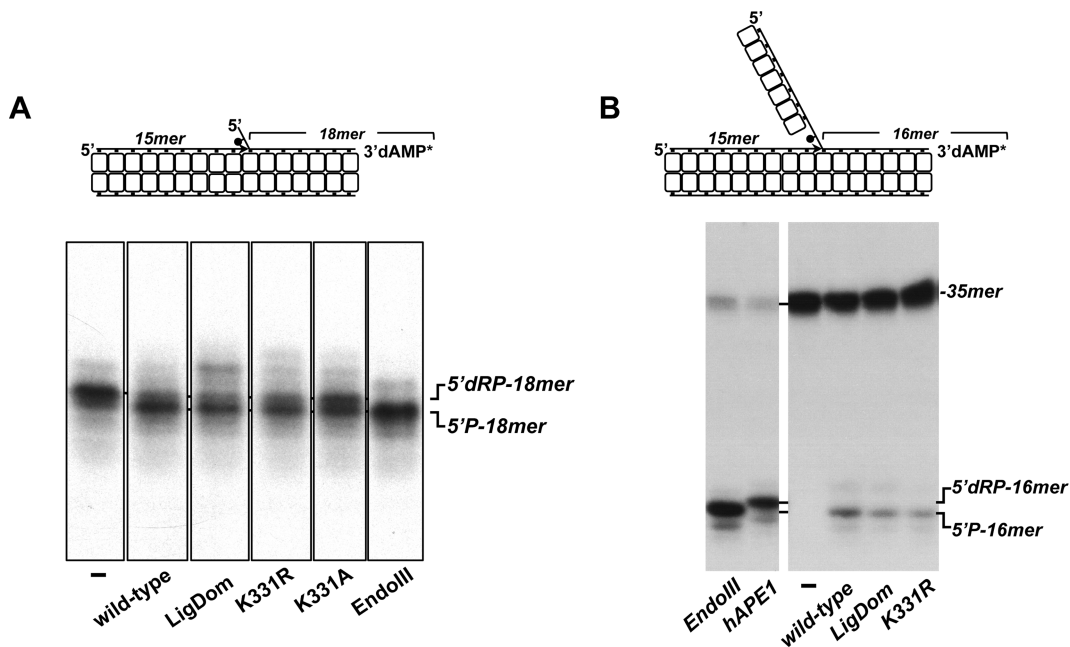
Figure 11. AP lyase activity of wild-type and *Bsu*LigD mutants on gap-filled BER intermediates and on flapped substrates. Top: schematic representation of the substrates used in the assay and corresponding to a filled gap with a dangling 5-dRP group in the downstream strand (**A**), and a flapped molecule where the 3′-end of the upstream strand is adjacent to the phosphodiester bond between the AP site and the next nucleotide in the downstream strand (**B**). The assays were performed as described in Materials and Methods. The substrates were previously incubated with *E. coli* UDG to create an AP site in nearly all DNA molecules. After incubation for 30 min at 30°C of 1 nM of the DNA substrate with 100 nM of either the wild-type, the indicated mutant enzyme or LigDom, samples were analyzed by 7M urea–20% PAGE and autoradiography, as described in Materials and Methods. When indicated, the DNA substrate was incubated with 0.2 U of either *h*APE1 or *E. coli* EndoIII. The positions of substrate and the products are indicated. Asterisks indicate the [^{32}P] labeled-3′ end. Full circle, AP site that results after treatment with *E. coli* UDG. The figures are composite images made from different parts of the same experiments.

SUPPLEMENTARY DATA

ACKNOWLEDGEMENTS

FUNDING

REFERENCES

1. Hoeijmakers,J.H. (2001) Genome maintenance mechanisms for preventing cancer. *Nature*, **411**, 366–374.
2. Pitcher,R.S., Brissett,N.C. and Doherty,A.J. (2007) Nonhomologous end-joining in bacteria: a microbial perspective. *Annu. Rev. Microbiol.*, **61**, 259–282.
3. Shuman,S. and Glickman,M.S. (2007) Bacterial DNA repair by non-homologous end joining. *Nat. Rev. Microbiol.*, **5**, 852–861.
4. Chang,H.H.Y., Pannunzio,N.R., Adachi,N. and Lieber,M.R. (2017) Non-homologous DNA end joining and alternative pathways to double-strand break repair. *Nat. Rev. Mol. Cell. Biol.*, **18**, 495–506.
5. Pannunzio,N.R., Watanabe,G. and Lieber,M.R. (2018) Nonhomologous DNA end-joining for repair of DNA double-strand breaks. *J. Biol. Chem.*, **293**, 10512–10523.
6. Aravind,L. and Koonin,E.V. (2001) Prokaryotic homologs of the eukaryotic DNA-end-binding protein Ku, novel domains in the Ku protein and prediction of a prokaryotic double-strand break repair system. *Genome Res.*, **11**, 1365–1374.
7. Bartlett,E.J., Brissett,N.C. and Doherty,A.J. (2013) Ribonucleolytic resection is required for repair of strand displaced nonhomologous end-joining intermediates. *Proc. Natl. Acad. Sci. U.S.A.*, **110**, E1984–E1991.
8. Iyer,L.M., Koonin,E.V., Leipe,D.D. and Aravind,L. (2005) Origin and evolution of the archaeo-eukaryotic primase superfamily and related palm-domain proteins: structural insights and new members. *Nucleic Acids Res.*, **33**, 3875–3896.
9. Weller,G.R. and Doherty,A.J. (2001) A family of DNA repair ligases in bacteria? *FEBS Lett.*, **505**, 340–342.
10. Cadet,J., Ravanat,J.L., TavernaPorro,M., Menoni,H. and Angelov,D. (2012) Oxidatively generated complex DNA damage: tandem and clustered lesions. *Cancer Lett.*, **327**, 5–15.
11. Datta,K., Neumann,R.D. and Winters,T.A. (2005) Characterization of complex apurinic/apyrimidinic-site clustering associated with an authentic site-specific radiation-induced DNA double-strand break. *Proc. Natl. Acad. Sci. U.S.A.*, **102**, 10569–10574.
12. Pogozelski,W.K. and Tullius,T.D. (1998) Oxidative strand scission of nucleic acids: routes initiated by hydrogen abstraction from the sugar moiety. *Chem. Rev.*, **98**, 1089–1108.
13. Ward,J.F. (1994) The complexity of DNA damage: relevance to biological consequences. *Int. J. Radiat. Biol.*, **66**, 427–432.
14. Ma,W., Resnick,M.A. and Gordenin,D.A. (2008) Apn1 and Apn2 endonucleases prevent accumulation of repair-associated DNA breaks in budding yeast as revealed by direct chromosomal analysis. *Nucleic Acids Res.*, **36**, 1836–1846.
15. Malyarchuk,S., Castore,R. and Harrison,L. (2008) DNA repair of clustered lesions in mammalian cells: involvement of non-homologous end-joining. *Nucleic Acids Res.*, **36**, 4872–4882.
16. Malyarchuk,S., Castore,R. and Harrison,L. (2009) Apex1 can cleave complex clustered DNA lesions in cells. *DNA Repair (Amst.)*, **8**, 1343–1354.
17. Yang,N., Galick,H. and Wallace,S.S. (2004) Attempted base excision repair of ionizing radiation damage in human lymphoblastoid cells produces lethal and mutagenic double strand breaks. *DNA Repair (Amst.)*, **3**, 1323–1334.
18. Datta,K., Purkayastha,S., Neumann,R.D., Pastwa,E. and Winters,T.A. (2011) Base damage immediately upstream from double-strand break ends is a more severe impediment to nonhomologous end joining than blocked 3′-termini. *Radiat. Res.*, **175**, 97–112.
19. Dobbs,T.A., Palmer,P., Maniou,Z., Lomax,M.E. and O'Neill,P. (2008) Interplay of two major repair pathways in the processing of complex double-strand DNA breaks. *DNA Repair (Amst.)*, **7**, 1372–1383.
20. Roberts,S.A., Strande,N., Burkhalter,M.D., Strom,C., Havener,J.M., Hasty,P. and Ramsden,D.A. (2010) Ku is a 5′-dRP/AP lyase that excises nucleotide damage near broken ends. *Nature*, **464**, 1214–1217.
21. de Ory,A., Zafra,O. and de Vega,M. (2014) Efficient processing of abasic sites by bacterial nonhomologous end-joining Ku proteins. *Nucleic Acids Res.*, **42**, 13082–13095.
22. Strande,N., Roberts,S.A., Oh,S., Hendrickson,E.A. and Ramsden,D.A. (2012) Specificity of the dRP/AP lyase of Ku promotes nonhomologous end joining (NHEJ) fidelity at damaged ends. *J. Biol. Chem.*, **287**, 13686–13693.
23. Strande,N.T., Carvajal-Garcia,J., Hallett,R.A., Waters,C.A., Roberts,S.A., Strom,C., Kuhlman,B. and Ramsden,D.A. (2014) Requirements for 5′dRP/AP lyase activity in Ku. *Nucleic Acids Res.*, **42**, 11136–11143.
24. Kosova,A.A., Khodyreva,S.N. and Lavrik,O.I. (2016) Ku antigen displays the AP lyase activity on a certain type of duplex DNA. *Biochim. Biophys. Acta*, **1864**, 1244–1252.
25. de Vega,M. (2013) The minimal *Bacillus subtilis* nonhomologous end joining repair machinery. *PLoS One*, **8**, e64232.
26. de Ory,A., Nagler,K., Carrasco,B., Raguse,M., Zafra,O., Moeller,R. and de Vega,M. (2016) Identification of a conserved 5′-dRP lyase activity in bacterial DNA repair ligase D and its potential role in base excision repair. *Nucleic Acids Res.*, **44**, 1833–1844.
27. Khodyreva,S.N., Ilina,E.S., Kutuzov,M.M., Sukhanova,M.V. and Lavrik,O.I. (2010) Poly(ADP-ribose) polymerase 1 interaction with apurinic/apyrimidinic sites. *Dokl. Biochem. Biophys.*, **431**, 69–72.
28. Pinz,K.G. and Bogenhagen,D.F. (2000) Characterization of a catalytically slow AP lyase activity in DNA polymerase gamma and other family A DNA polymerases. *J. Biol. Chem.*, **275**, 12509–12514.
29. Prasad,R., Beard,W.A., Strauss,P.R. and Wilson,S.H. (1998) Human DNA polymerase beta deoxyribose phosphate lyase. Substrate specificity and catalytic mechanism. *J. Biol. Chem.*, **273**, 15263–15270.
30. Takao,M., Oohata,Y., Kitadokoro,K., Kobayashi,K., Iwai,S., Yasui,A., Yonei,S. and Zhang,Q.M. (2009) Human Nei-like protein NEIL3 has AP lyase activity specific for single-stranded DNA and confers oxidative stress resistance in *Escherichia coli* mutant. *Genes Cells*, **14**, 261–270.
31. Piersen,C.E., McCullough,A.K. and Lloyd,R.S. (2000) AP lyases and dRPases: commonality of mechanism. *Mutat. Res.*, **459**, 43–53.
32. Kibbe,W.A. (2007) OligoCalc: an online oligonucleotide properties calculator. *Nucleic Acids Res.*, **35**, W43–W46.
33. David,S.S. and Williams,S.D. (1998) Chemistry of Glycosylases and Endonucleases Involved in Base-Excision Repair. *Chem. Rev.*, **98**, 1221–1262.
34. Khodyreva,S. and Lavrik,O.I. (2011) In: Chen,CC (ed). *Selected Topics in DNA Repair*. InTech, pp. 305–330.
35. McCullough,A.K., Dodson,M.L. and Lloyd,R.S. (1999) Initiation of base excision repair: glycosylase mechanisms and structures. *Annu. Rev. Biochem.*, **68**, 255–285.
36. Williams,S.D. and David,S.S. (1998) Evidence that MutY is a monofunctional glycosylase capable of forming a covalent Schiff base intermediate with substrate DNA. *Nucleic Acids Res.*, **26**, 5123–5133.
37. Krwawicz,J., Arczewska,K.D., Speina,E., Maciejewska,A. and Grzesiuk,E. (2007) Bacterial DNA repair genes and their eukaryotic homologues: 1. Mutations in genes involved in base excision repair (BER) and DNA-end processors and their implication in mutagenesis and human disease. *Acta Biochim. Pol.*, **54**, 413–434.

38. Brissett,N.C., Martin,M.J., Bartlett,E.J., Bianchi,J., Blanco,L. and Doherty,A.J. (2013) Molecular basis for DNA double-strand break annealing and primer extension by an NHEJ DNA polymerase. *Cell Rep.*, **5**, 1108–1120.

39. Brissett,N.C., Martin,M.J., Pitcher,R.S., Bianchi,J., Juarez,R., Green,A.J., Fox,G.C., Blanco,L. and Doherty,A.J. (2011) Structure of a preternary complex involving a prokaryotic NHEJ DNA polymerase. *Mol. Cell*, **41**, 221–231.

40. Gelfand,C.A., Plum,G.E., Grollman,A.P., Johnson,F. and Breslauer,K.J. (1998) Thermodynamic consequences of an abasic lesion in duplex DNA are strongly dependent on base sequence. *Biochemistry*, **37**, 7321–7327.

41. Minetti,C.A., Sun,J.Y., Jacobs,D.P., Kang,I., Remeta,D.P. and Breslauer,K.J. (2018) Impact of bistrand abasic sites and proximate orientation on DNA global structure and duplex energetics. *Biopolymers*, **109**, e23098.

42. Brissett,N.C., Pitcher,R.S., Juarez,R., Picher,A.J., Green,A.J., Dafforn,T.R., Fox,G.C., Blanco,L. and Doherty,A.J. (2007) Structure of a NHEJ polymerase-mediated DNA synaptic complex. *Science*, **318**, 456–459.

43. Rydberg,B. and Game,J. (2002) Excision of misincorporated ribonucleotides in DNA by RNase H (type 2) and FEN-1 in cell-free extracts. *Proc. Natl. Acad. Sci. U.S.A.*, **99**, 16654–16659.

44. Matsumoto,Y. and Kim,K. (1995) Excision of deoxyribose phosphate residues by DNA polymerase beta during DNA repair. *Science*, **269**, 699–702.

45. Bebenek,K., Tissier,A., Frank,E.G., McDonald,J.P., Prasad,R., Wilson,S.H., Woodgate,R. and Kunkel,T.A. (2001) 5′-Deoxyribose phosphate lyase activity of human DNA polymerase iota in vitro. *Science*, **291**, 2156–2159.

46. Garcia-Diaz,M., Bebenek,K., Kunkel,T.A. and Blanco,L. (2001) Identification of an intrinsic 5′-deoxyribose-5-phosphate lyase activity in human DNA polymerase lambda: a possible role in base excision repair. *J. Biol. Chem.*, **276**, 34659–34663.

47. Prasad,R., Longley,M.J., Sharief,F.S., Hou,E.W., Copeland,W.C. and Wilson,S.H. (2009) Human DNA polymerase theta possesses 5′-dRP lyase activity and functions in single-nucleotide base excision repair in vitro. *Nucleic Acids Res.*, **37**, 1868–1877.

48. Bogenhagen,D.F. and Pinz,K.G. (1998) The action of DNA ligase at abasic sites in DNA. *J. Biol. Chem.*, **273**, 7888–7893.

49. Pinz,K.G. and Bogenhagen,D.F. (1998) Efficient repair of abasic sites in DNA by mitochondrial enzymes. *Mol. Cell Biol.*, **18**, 1257–1265.

50. Pitcher,R.S., Brissett,N.C., Picher,A.J., Andrade,P., Juárez,R., Thompson,D., Fox,G.C., Blanco,L. and Doherty,A.J. (2007) Structure and function of a mycobacterial NHEJ DNA repair polymerase. *J. Mol. Biol.*, **366**, 391–405.

51. Mahajan,K.N., Nick McElhinny,S.A., Mitchell,B.S. and Ramsden,D.A. (2002) Association of DNA polymerase mu (pol mu) with Ku and ligase IV: role for pol mu in end-joining double-strand break repair. *Mol. Cell Biol.*, **22**, 5194–5202.

52. Zhu,H. and Shuman,S. (2010) Gap filling activities of *Pseudomonas* DNA ligase D (LigD) polymerase and functional interactions of LigD with the DNA end-binding Ku protein. *J. Biol. Chem.*, **285**, 4815–4825.

53. Bebenek,K., Pedersen,L.C. and Kunkel,T.A. (2014) Structure-function studies of DNA polymerase lambda. *Biochemistry*, **53**, 2781–2792.

54. Garcia-Diaz,M., Bebenek,K., Gao,G., Pedersen,L.C., London,R.E. and Kunkel,T.A. (2005) Structure-function studies of DNA polymerase lambda. *DNA Repair (Amst.)*, **4**, 1358–1367.